

RESEARCH

Open Access



Reducing severity of inflammatory bowel disease through colonization of *Lactiplantibacillus plantarum* and its extracellular vesicles release

Yuanyuan Wu^{1†}, Xinyue Huang^{1†}, Qianbei Li^{1†}, Chaoqun Yang^{1,2†}, Xixin Huang¹, Hualongyue Du¹, Bo Situ^{1*}, Lei Zheng^{1*} and Zihao Ou^{1*}

Abstract

Inflammatory bowel disease (IBD) is characterized by compromised intestinal barrier function and a lack of effective treatments. Probiotics have shown promise in managing IBD due to their ability to modulate the gut microbiota, enhance intestinal barrier function, and exert anti-inflammatory effects. However, the specific mechanisms through which probiotics exert these therapeutic effects in IBD treatment remain poorly understood. Our research revealed a significant reduction of *Lactiplantibacillus plantarum* (*L. plantarum*) in the gut microbiota of IBD patients. *L. plantarum* is a well-known probiotic strain in the list of edible probiotics, recognized for its beneficial effects on gut health, including its ability to strengthen the intestinal barrier and reduce inflammation. We demonstrated that supplementation with *L. plantarum* could alleviate IBD symptoms in mice, primarily by inhibiting apoptosis in intestinal epithelial cells through *L. plantarum*'s bacterial extracellular vesicles (*L. plant*-EVs). This protective effect is dependent on the efficient uptake of *L. plant*-EVs by intestinal cells. Intriguingly, watermelon enhances *L. plantarum* colonization and *L. plant*-EVs release, further promoting intestinal barrier repair. Our findings contribute to the understanding of *L. plant*-EVs in the probiotic-based therapeutic approach for IBD, as they are promising candidates for nanoparticle-based therapeutic methods that are enhanced by natural diets such as watermelon. This study thereby offers a potential breakthrough in the management and treatment of IBD.

[†]Yuanyuan Wu, Xinyue Huang, Qianbei Li and Chaoqun Yang contributed equally to this work.

*Correspondence:

Bo Situ

bositu@smu.edu.cn

Lei Zheng

nfyyzhenglei@smu.edu.cn

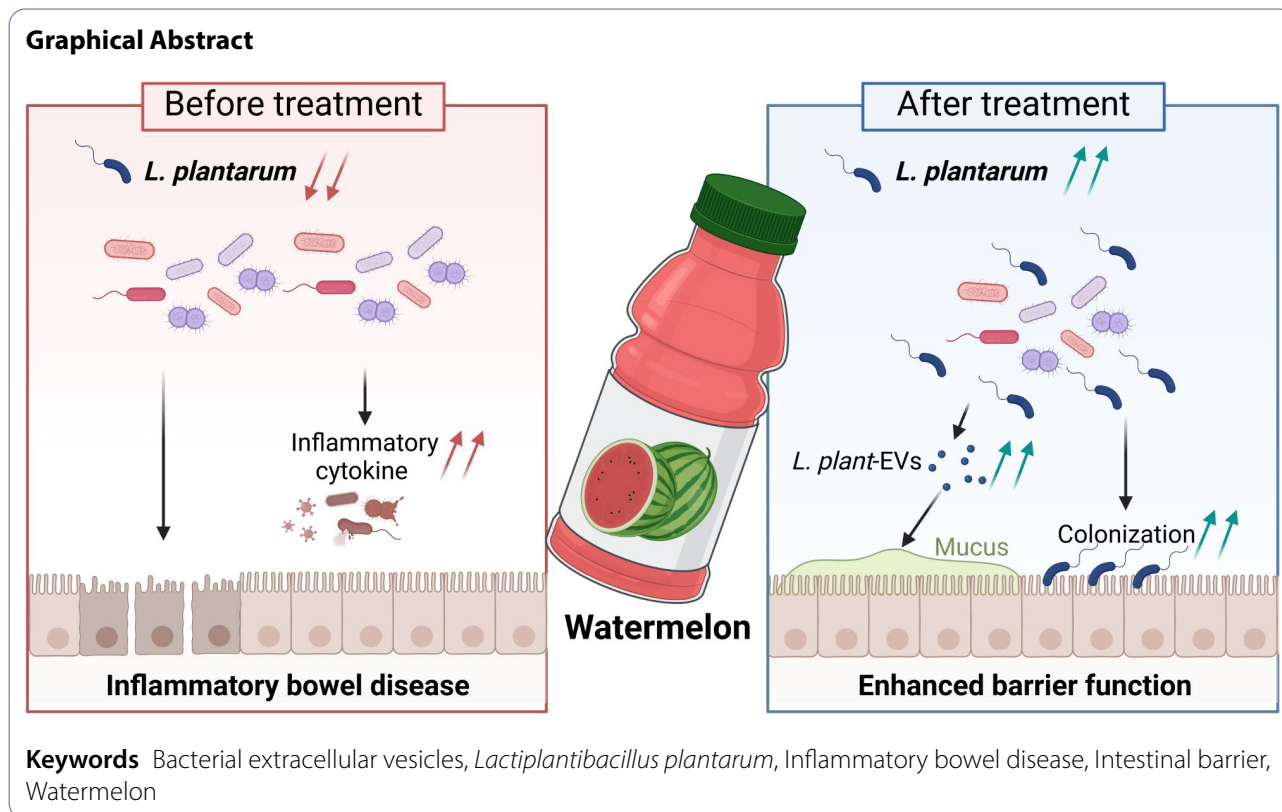
Zihao Ou

ozh_xnp@smu.edu.cn

Full list of author information is available at the end of the article



© The Author(s) 2025. **Open Access** This article is licensed under a Creative Commons Attribution-NonCommercial-NoDerivatives 4.0 International License, which permits any non-commercial use, sharing, distribution and reproduction in any medium or format, as long as you give appropriate credit to the original author(s) and the source, provide a link to the Creative Commons licence, and indicate if you modified the licensed material. You do not have permission under this licence to share adapted material derived from this article or parts of it. The images or other third party material in this article are included in the article's Creative Commons licence, unless indicated otherwise in a credit line to the material. If material is not included in the article's Creative Commons licence and your intended use is not permitted by statutory regulation or exceeds the permitted use, you will need to obtain permission directly from the copyright holder. To view a copy of this licence, visit <http://creativecommons.org/licenses/by-nc-nd/4.0/>.



Introduction

Inflammatory bowel disease (IBD), a chronic inflammatory disorder affecting millions of people worldwide, has a complex pathogenesis involving genetic, environmental, and immunological factors [1]. These elements contribute to disrupt key processes such as epithelial cell function, intestinal permeability, immune response regulation, and the gut microbiota balance, ultimately leading to compromised intestinal dysfunction [2]. Despite existing treatments, sustained removal or complete recovery in IBD patients remains elusive, largely owing to the limited understanding of its pathogenesis and the constraints of current drugs [3, 4]. Probiotics have emerged as a promising approach to manage gut microbiota and maintain internal barrier homeostasis [5, 6]. Strains such as *Lactocaseibacillus rhamnosus* and *Lactiplantibacillus reuteri* improve barrier function by upregulating tight junction proteins, which are crucial for preventing the entry of harmful substances into the bloodstream [7, 8]. However, the efficacy of specific probiotics in IBD treatment remains uncertain, with challenges in achieving sustained colonization and stable therapeutic outcomes. Moreover, the key active components and mechanisms underlying probiotics' action in IBD are not fully understood.

Recent research has increasingly focused on bacterial extracellular vesicles (BEVs) as crucial mediators of bacterial-host interactions and the progression of

diseases [9–11]. These nanoscale particles, ranging from 30 to 200 nm in size, are carriers of bioactive molecules like proteins and genetic material [12, 13]. Notably, BEVs [14], owing to their specific structural properties, exhibit enhanced stability within the human gastrointestinal tract, effectively resisting degradation by digestive enzymes and being readily assimilated by host cells [15, 16]. Moreover, probiotic-derived BEVs have been identified to possess anti-inflammatory, antioxidant, and immunomodulatory properties, marking them as promising candidates in the realm of nanoparticle drug for disease treatment [17–19]. Therefore, deciphering the role of these nanoscale particles in probiotic-mediated gut barrier regulation could lead to breakthrough BEV-based IBD treatments, particularly in terms of enhancing BEV production and nanoparticle-based therapeutic methods.

In this study, we report a significantly reduced presence of *L. plantarum* in the gut microbiota of IBD patients, and supplementation with *L. plantarum* could alleviate IBD symptoms in a mouse model. We demonstrated that *L. plantarum* is capable of inhibiting apoptosis in intestinal epithelial cells *via* the mPTP-CytC-Caspase-9-Caspase-3 pathway, which is mediated through the release of its BEVs. Furthermore, watermelon was found to act as a catalyst, enhancing the growth of *L. plantarum* and the secretion of *L. plant-EVs*, which contributes to the alleviation of IBD symptoms. This study underscored the

clinical significance of *L. plant*-EVs in preserving intestinal barrier integrity, positioning them as potential candidates for nanoparticle-based therapeutic strategies. Crucially, the effectiveness of these vesicles is significantly enhanced by watermelon, offering a unique and synergistic approach to IBD therapy.

Method

Animals and the IBD model

All mouse experiments in this study were approved by the Committee on the Use of Live Animals in Teaching and Research at the Southern Medical University (approval number: SMUL2022002) and were performed following the Guidelines for Care and Use of Laboratory Animals of Southern Medical University. Specific pathogen-free (SPF) healthy male C57BL/6J mice (6–8 week-old) were procured from Guangdong Zhiyuan Biomedical Technology Co., Ltd. and housed in the SPF animal facility of Southern Medical University. The mice were maintained under constant temperature, humidity, and 12/12 h light/dark cycle conditions and provided ad libitum access to food and water.

After 1 week of adaptation, the mice in the IBD model group were allowed free access to a 3% DSS aqueous solution (MB5535, meilunbio) for 7 days. Mice were treated with 300 μ L of PBS or other interventions such as *E. coli* (10^9 CFU/mL), *E. coli*-EVs (30 μ g), *L. plantarum* (10^9 CFU/mL), *L. plant*-EVs (30 μ g) and watermelon supernatant each day as the control or experimental groups.

A mixture of vancomycin hydrochloride (10 mg/mL, 200 μ L, V820413, Macklin), metronidridin (10 mg/mL, 200 μ L, M813526, Macklin), neomycin (20 mg/mL, 200 μ L, XY-K1226, X-Y Biotechnology) and ampicillin (20 mg/mL, 200 μ L, A830931, Macklin) was used for 7 days to clear the gut microbiota of the mice.

Cell culture

Human normal colonic epithelial (NCM 460) cells were cultured in Dulbecco's modified Eagle medium (DMEM, C11995500BT, Gibco) supplemented with 10% fetal bovine serum (FBS, 164210-50, Procell), 10 U/mL penicillin (PB180120, Procell), and 0.1 mg/mL streptomycin (PB180120, Procell). The cells were maintained at 37 °C with 5% CO₂ in an incubator.

Cell scratching assay

NCM 460 cells were plated at 2.5×10^5 /well in a 12-well plate. After the cells had adhered overnight, 2 scratches per well were made with a 200 μ L pipet tip. Then, the cells were washed twice with PBS. Next, 1 mL of serum-free medium containing 3% DSS and 10 μ g/mL *L. plant*-EVs or *E. coli*-EVs was added to each well. Cell migration was evaluated at 0 h, 12 h and 24 h with a Nikon inverted microscope, and the scratch areas were quantified with ImageJ software.

Western blot

NCM 460 cells were plated at 3.5×10^5 /well in a 6-well plate. After they had allowed to adhere overnight, the cells were washed twice with PBS. Subsequently, 2 mL of serum-free medium containing 3% DSS and different concentrations of *L. plant*-EVs (5, 10, 15, 20 μ g/mL) was added to each well. The cells were cultured with *L. plant*-EVs for 0 h, 12 h and 24 h. Then, protein samples from NCM 460 cells were obtained via RIPA lysis buffer (WB3100, NCM Biotech) containing 1% protease and phosphatase inhibitor cocktail phenylmethanesulfonyl fluoride (P002, NCM Biotech). The total protein concentration was determined using the BCA Protein Assay Kit (FD2001, Fdbio Science). Equal amounts of proteins (30 μ g per group) were loaded for 4–20% Protein Pre made Gel (ET15420Gel, ACE Biotechnology) and subjected to electrophoresis. After transferring protein to polyvinylidene difluoride (PVDF) membranes, the blots were blocked with 5% Bovine Serum Albumin (BSA, FD0030, Fdbio Science) for 2 h at room temperature. The membranes were incubated with primary antibodies overnight at 4 °C, and then with the corresponding secondary antibodies for 2 h at room temperature. All primary antibodies were obtained from Affinity Biosciences. All secondary antibodies were obtained from Fdbio science. GAPDH (ab201822, Abcam) and β -tubulin (AF7011, Affinity Biosciences) was used for normalization. The bands were quantified using ImageJ software.

Bacterial DNA extraction

DNA extraction from all fecal samples was performed via QIAamp Fast DNA Stool Mini Kit (51604, Qiagen) with a modified protocol following the manufacturer's instructions specific for the fecal samples. The quantity and purity of all the extracted DNA were checked with a NanoDrop ND-1000 Spectrophotometer (Thermo Fisher Scientific) and then stored at –20 °C.

Quantitative real-time PCR (qRT-PCR)

The total cellular RNA was extracted by using TRIzol agent (15596026, Invitrogen) and synthesized into cDNA via a reverse transcription kit (RR036A, Takara). Subsequently, the SYBR[®] Green Pro Taq HS Premix (AG11701, Accurate Biology) was added for gene expression analysis. The primers used for qRT-PCR are described Table S1.

Annexin V/PI staining and cell cycle detection

NCM 460 cells were plated at 3.5×10^5 /well in a 6-well plate. After they had allowed to adhere overnight, the cells were washed twice with PBS. Subsequently, 2 mL of serum-free medium containing 3% DSS, different concentrations of *L. plant*-EVs (5, 10, 15, 20 μ g/mL) and PBS

was added to each well. The cells were cocultured with *L. plant*-EVs for 0 h, 12 h, 24 h.

An Annexin V-fluorescein isothiocyanate (FITC)/propidium iodide (PI) Apoptosis Detection Kit (40302ES50, Yeasen Biotechnology) was used to identify apoptotic and necrotic cells. Following the manufacturer's instructions, $1-5 \times 10^5$ live cells were harvested and stained (10 μ L PI and 5 μ L Annexin V-FITC) for 15 min in the dark at room temperature, before analysis via the BD Fortessa multidimensional high-definition flow cytometer. In the resulting dot plots, the X-axis represents the intensity of green fluorescence (Annexin V), and the Y-axis represents the intensity of red fluorescence (PI). The cell population distribution analysis was divided into four quadrants: Annexin V-/PI-, Annexin V+/PI-, Annexin V-/PI+, and Annexin V+/PI+ represented the normal state, early apoptosis, necrosis, and late apoptosis, respectively.

Enzyme-linked immunosorbent assay

Protein samples from NCM 460 cells were obtained using RIPA lysis buffer containing 1% protease and phosphatase inhibitors. MPTP protein levels were measured by using the Human MPTP ELISA Kit (DG12601H, Dogesce).

Bacterial growth condition

E. coli was grown at 37 °C in Luria-Bertani (LB) Broth (HB0128, Hopebio) with continuous shaking at 160 rpm for 18 h. *L. plantarum* was grown anaerobically at 37 °C in de Man, Rogosa and Sharpe (MRS) broth (HB0384-1, Hopebio) supplemented with 1% D-(+)-Maltose monohydrate (D813131, Macklin) and 1% yeast extract (050090, HuanKai Biology) for 12 h.

Fruits supernatant promoted bacterial growth

The MRS broth was supplemented with 1% cysteine and 1% PBS, or the supernatant of fruits such as pitaya, peach, and watermelon. *L. plantarum* was inoculated into the medium, and after 2, 4, 8, 12, and 24 h of culture, the bacterial culture was centrifuged at $3,000 \times g$ for 10 min. After removing the supernatant, an equivalent volume of PBS was added to resuspend the bacteria, and the OD600 values were measured.

Watermelon supernatant promoted the release of BEVs

The MRS broth was supplemented with 1% cysteine, 1% PBS, or watermelon supernatant. *L. plantarum* was then inoculated into the medium and cultured for 8 h. *L. plant*-EVs were isolated by ultracentrifugation, and protein quantification was performed using the BCA Protein Assay Kit.

Isolation of BEVs

BEVs were isolated from the bacterial culture. The bacteria were first removed by centrifugation at $300 \times g$ for 10 min, then $3,000 \times g$ for 20 min, and finally $12,000 \times g$ for 30 min at 4 °C. The supernatants were further filtered with a 0.22 μ m pore-sized filter, removing residual bacteria and cellular debris. BEVs were isolated by ultracentrifugation of the filtrate at $135,000 \times g$ for 70 min at 4 °C and resuspended in PBS. BEV samples were stored at -80 °C for subsequent studies. The protein quantification of BEVs was performed with the BCA Protein Assay Kit.

Characterization of BEVs

The morphology and the size distribution of *L. plant*-EVs were observed by Transmission electron microscope (H-7650, Hitachi) and Nanoparticles tracking analysis (ZetaView PMX-120, Particle Metrix). The surface marker LTA (MA1-7402, Thermo Fisher Scientific) of *L. plant*-EVs was characterized by Western blot.

16S rRNA gene sequencing

16S rRNA sequencing was performed at Novogene (Beijing, China) using NovaSeq 6000 system. Total DNA was extracted from human fecal samples and stored at -80°C. Later, the content of the extracted total DNA was quantified by Nanodrop, and the quality was checked by 1% agarose gel electrophoresis. For 16S amplicon sequencing, the variable V4 region of bacterial 16S rRNA was amplified with the primers V4F (5'-GTGTGYCAGC-MGCCGCGGTAA-3') and V4R (5'-CCGGACTAC-NVGGGTWCTAAT-3') and the PCR products were purified with a GeneJET Gel Extraction Kit (K0691, Thermo Scientific). Sequencing libraries were generated using Illumina TruSeq DNA PCR-Free Library Preparation Kit (Illumina) and index codes were added. At last, the library was sequenced on an Illumina NovaSeq platform and 250 bp paired-end reads were generated. Sequence denoising, or operational taxonomic unit (OTU) clustering, was performed in line with the QIIME2 dada2 analysis process or the analysis process of Vsearch software. At the amplicon sequence variant (ASV)/OTU level, the distance matrix of each sample was calculated, and the differences in diversity and the significance of differences among different samples (groups) were measured by various unsupervised sorting and clustering methods, combined with the corresponding statistical tests such as PERMANOVA, ANOSIM, and PERMDISP.

RNA sequencing and analysis

RNA samples from NCM 460 cells were obtained using AG RNAex Pro Reagent (AG21102, Accurate Biotechnology). Total amounts and integrity of the RNA were assessed using the RNA Nano 6000 Assay Kit of the

Bioanalyzer 2100 system (Agilent Technologies, CA, USA). After the library was qualified, the different libraries were pooling according to the effective concentration and the target amount of data off the machine, then being sequenced by the Illumina NovaSeq 6000. The end reading of 150 bp pairing was generated. The image data measured by the high-throughput sequencer were converted into sequence data (reads) by CASAVA base recognition. We downloaded the reference genome and gene model annotation files from the GENCODE database (<https://www.genecodegenes.org>). Index of the reference genome was built via HISAT2 (v2.0.5) and paired-end clean reads were aligned to the reference genome via HISAT2 (v2.0.5). FeatureCounts (v1.5.0-p3) was used to count the reads numbers mapped to each gene. Differential expression analysis was performed using the DESeq2 R package (1.20.0). Gene Ontology (GO) enrichment analysis of the differentially expressed genes was implemented by the clusterProfiler R package (3.8.1).

Clinical samples

Healthy donors and colitis patients

The sample collection protocol was approved by the Ethics Committee of Nanfang Hospital, Southern Medical University (approval number: NFEC-2022-001). Healthy donors and colitis patients were selected from Nanfang hospital according to standard guidelines [31]. All the stool samples were stored at -80°C .

Volunteers

Volunteers were asked to eat fast fruit for 3 days and stool samples were collected. Then, they were assigned to eat fresh watermelon for 7 days and stool samples were collected again. The feces before and after watermelon consumption were paired and stored at -80°C . The sample collection was approved by the Ethics Committee of Nanfang Hospital, Southern Medical University (approval number: NFEC-2022-001).

Statistical analysis

All data were presented as mean \pm standard deviation (SD). One-way analysis of variance (ANOVA) was used for comparisons among multiple groups. Student's t-test was used for comparisons between two groups. When the data did not pass the normality and lognormality tests, the Mann Whitney test was used for comparisons between two groups, while the Kruskal-Wallis test was used for comparisons among multiple groups. All the statistical analyses were conducted using GraphPad Prism 9.0. P value of <0.05 was considered statistically significant. $*P < 0.05$, $**P < 0.01$, $***P < 0.001$, and $****P < 0.0001$.

Results

Lactiplantibacillus plantarum supplementation reduced symptoms of IBD

To investigate the potentially beneficial microbiota associated with to IBD, we collected fecal samples from IBD patients for 16 S rRNA sequencing to characterize the composition of the intestinal microbiota (Fig. 1a). All patients in the study diagnosed with IBD were confirmed through colonoscopy and subsequent pathological analysis of tissue samples (Fig. 1b). To control for potential confounding factors such as dietary differences and regional variations, we conducted comparative analyses using additional public databases (the Human Microbiome Project (HMP) Database). Notably, we found a lower abundance of *L. plantarum* in the feces of IBD patients compared to healthy individuals (Fig. 1c), suggesting the poor colonization by *L. plantarum* under IBD conditions.

To assess the effects of *L. plantarum* supplementation on IBD, 6–8 week-old mice were allowed free access to a 3% DSS aqueous solution for 7 days to construct an IBD mouse model (Fig. 1d). The mice were then divided into three groups: the first group received only PBS (blank group), the second group was administered *Escherichia coli* (*E. coli*), a common gut bacterium (control group), and the third group was treated with *L. plantarum* (Fig. 1d). *L. plantarum* supplementation effectively alleviated DSS-induced weight loss (Fig. 1e and f) and colon shortening (Fig. 1g) compared with those in PBS group, whereas *E. coli* supplementation did not produce similar benefits. Hematoxyli-eosin (H&E) staining indicated that *L. plantarum* treatment reduced inflammatory cell infiltration and mucosal damage in the colon (Fig. 1h). These findings were corroborated by Alcian blue-periodic acid-Schiff (AB-PAS) staining, which showed that *L. plantarum* markedly restored mucus secretion in goblet cells, diminished by DSS, an effect not seen with *E. coli* treatment (Fig. 1h and i). Additionally, immunofluorescence analysis of mucosal barrier protein expression in tissue samples revealed that *L. plantarum* stabilized the expression of tight junction proteins, including ZO-1 (Fig. 1h and j), Occludin (Fig. 1h and k) and E-cadherin (Fig. 1h and l). *L. plantarum* increased E-cadherin and ZO-1 levels, as determined by Western blot (Fig. 1m and Figure S1a-c) and qPCR (Figure S1e-g) while *L. plantarum* had a substantial effect on gene expression with notable increases in Ecadherin, Occludin, and ZO-1 expression. Collectively, these findings indicate that the administration of *L. plantarum* significantly reduces inflammatory responses, and mucosal damage in a mouse model of IBD.

L. plant-EVs alleviated IBD symptoms in mice

EVs derived from bacteria have emerged as a promising approach to modulate human pathophysiology in

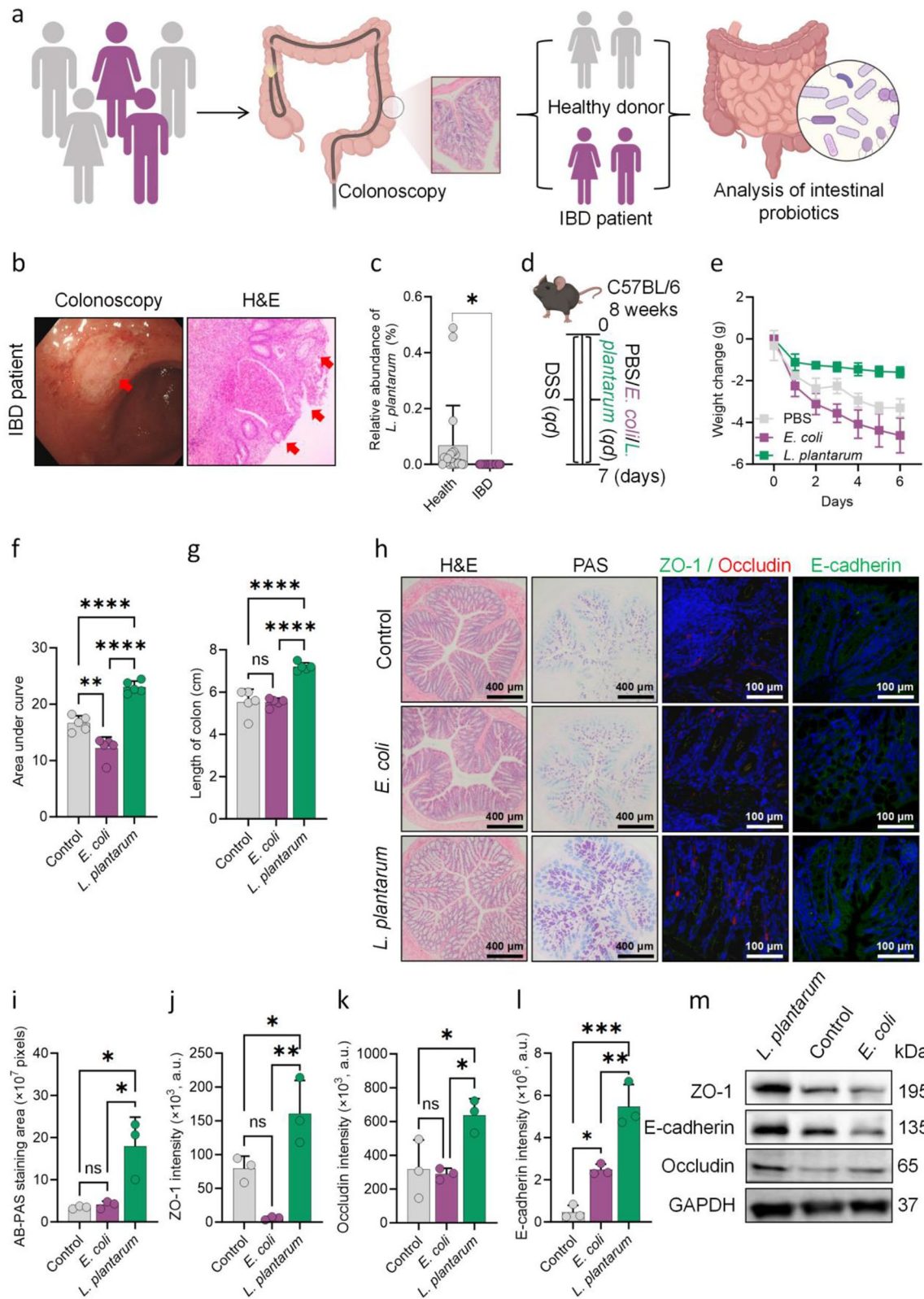


Fig. 1 (See legend on next page.)

(See figure on previous page.)

Fig. 1 Alleviation of Intestinal Barrier Dysfunction by *L. plantarum*. **(a)** Collection of fecal samples from patients. **(b)** Colonoscopy and histological examination of patient tissue samples. **(c)** Measurement of the relative abundance of *L. plantarum* in the human gut via 16 S rRNA sequencing (IBD $n=20$, NC $n=20$). **(d)** Flow chart illustrating the protocol for treating colitis mice with *L. plantarum*. **(e, f)** Daily weight changes and area under the curve analyses in mice ($n=5$). **(g)** Measurement of colon length in each experimental group ($n=5$). **(h)** H&E stained colon sections, AB-PAS stained inner mucus layers of colon sections, and immunofluorescence staining for intestinal epithelial tight junction proteins. **(i-l)** Quantitative analyses of the mucus content secreted by goblet cells and the expression levels of the tight junction proteins Occludin, ZO-1, and E-cadherin ($n=3$). **(m)** Expression of the gut barrier-associated proteins Ecadherin, Occludin, and ZO-1 in colon tissues of control, *E. coli*-treated and *L. plantarum*-treated mice by Western blot in a mouse model of IBD. Student's *t* test was used to calculate the *P* values in **(c)**. One-way ANOVA was used to calculate the *P* values in **(f-g)** and **(i-l)**. * $P < 0.05$, ** $P < 0.01$, *** $P < 0.001$, and **** $P < 0.0001$

recent years [20]. These nano-particles derived from intestinal commensal bacteria display remarkable stability and resistance to digestive enzymes in the gut [21]. Furthermore, they are readily taken up by host cells [22]. Therefore, these vesicles may play crucial roles as key mediators in the beneficial effects of probiotics [23]. We aimed to investigate the role of *L. plant*-EVs in IBD. *L. plant*-EVs were isolated from the culture media via by ultracentrifugation and characterized by Nanoparticle tracking analysis (NTA), Western blot (WB) and Transmission electron microscopy (TEM) (Figure S2a-c). The collected particles ranged from 40 nm to 500 nm in size (Figure S2a) and expressed lipoteichoic acid (LTA), the marker substance of gram-positive bacteria (Figure S2b). Moreover, their spherical shape was illustrated by TEM (Figure S2c), which suggested the successful separation of high-purity *L. plant*-EVs.

To delve deeper into the role of *L. plant*-EVs in microbe-host interactions (Fig. 2a), we explored their uptake by host cells. We incubated the EVs with NCM 460 cells for 3 h. The absorption of the fluorescence signal by these cells, particularly its accumulation around the perinuclear region, implies that *L. plant*-EVs could influence cell function (Fig. 2b). To evaluate the effect of *L. plant*-EVs, we conducted scratch tests using NCM 460 cells incubated with *L. plant*-EVs or *E. coli*-EVs. IBD cell models were induced using 3% DSS and divided into three groups: a blank control with PBS, a negative control with *E. coli*-EVs, and a treatment group with *L. plant*-EVs. The results confirmed the migration potential of NCM 460 cells treated with *L. plant*-EVs was greater than that of cells treated with *E. coli*-EVs or PBS after 12–24 h of co-culture (Fig. 2c and d). Subsequently, the effects of *L. plant*-EVs were also observed in vivo (Fig. 2e). Compared with the other groups, *L. plant*-EVs showed a trend of alleviating body weight loss (Fig. 2f and g) and improving colon shortening (Fig. 2h) in the IBD mouse model, although without reaching statistical significance. H&E and AB-PAS staining revealed that pathological features induced by DSS were restored by *L. plant*-EVs (Fig. 2i and j). In contrast, the *E. coli*-EVs group still exhibited moderate inflammatory cell infiltration and decreased mucus secretion (Fig. 2i and j). Immunofluorescence analysis further revealed significantly increased expression of Occludin and E-cadherin in the *L. plant*-EVs group

compared to the other two groups (Fig. 2i, l-m), even though the expression of ZO-1 remained unchanged significantly (Fig. 2i, k). Additionally, *L. plant*-EVs markedly elevated the levels of E-cadherin, occludin, and ZO-1, as confirmed by Western blot (Fig. 2n and Figure S3a-c) and qPCR (Figure S3d-f), indicating that *L. plant*-EVs promote intestinal barrier function. Overall, the data suggested that *L. plant*-EVs were the key component in the effect of *L. plantarum* to alleviate IBD.

***L. plant*-EVs inhibited intestinal epithelial cell apoptosis via mPTP-CytC-caspase-9-caspase-3 axis**

After confirming the ability of *L. plant*-EVs to mitigate IBD, we aimed to further investigate the underlying mechanism. Transcriptomic analysis was performed on extracted RNAs from 3% DSS treated intestinal epithelial cells after 24 h of incubation with *L. plant*-EVs. The results showed the main differentially expressed genes (DEGs), with 483 genes whose expression was altered in the control group, 425 genes in the *L. plant*-EVs treatment group, and a total of 11,694 genes whose expression changed between the two groups (Fig. 3a). The volcano plot results indicated that among the analyzed genes, 1708 genes showed significant upregulation, while 2081 genes demonstrated significant downregulation (Fig. 3b). Additionally, the distinction between the control and *L. plant*-EVs treatments was evident in an unsupervised hierarchical clustering analysis (Fig. 3c). Analysis of differentially expressed genes associated with apoptosis revealed a distinct pattern, indicating that *L. plant*-EVs treatment may contribute to the amelioration of apoptosis (Fig. 3d). This evidence indicated that *L. plant*-EVs treatment may reduce apoptosis, potentially through transcriptional remodeling. We observed a notable decrease in the expression levels of mPTP in the colon of the *L. plant*-EVs group, corroborating our hypothesis (Fig. 3e). To investigate whether *L. plant*-EVs regulate apoptosis through the mPTP-CytC-Caspase pathway, we evaluated the expression levels of key apoptotic proteins in cells treated with increasing concentrations (5, 10, 15, and 20 $\mu\text{g/mL}$) of *L. plant*-EVs. As the concentration of *L. plant*-EVs increased, the expression of cytochrome C (CytC), Cleaved-Caspase 3, and Cleaved-Caspase 9 showed a decreasing trend, providing further evidence that *L. plant*-EVs effectively alleviate apoptosis via the

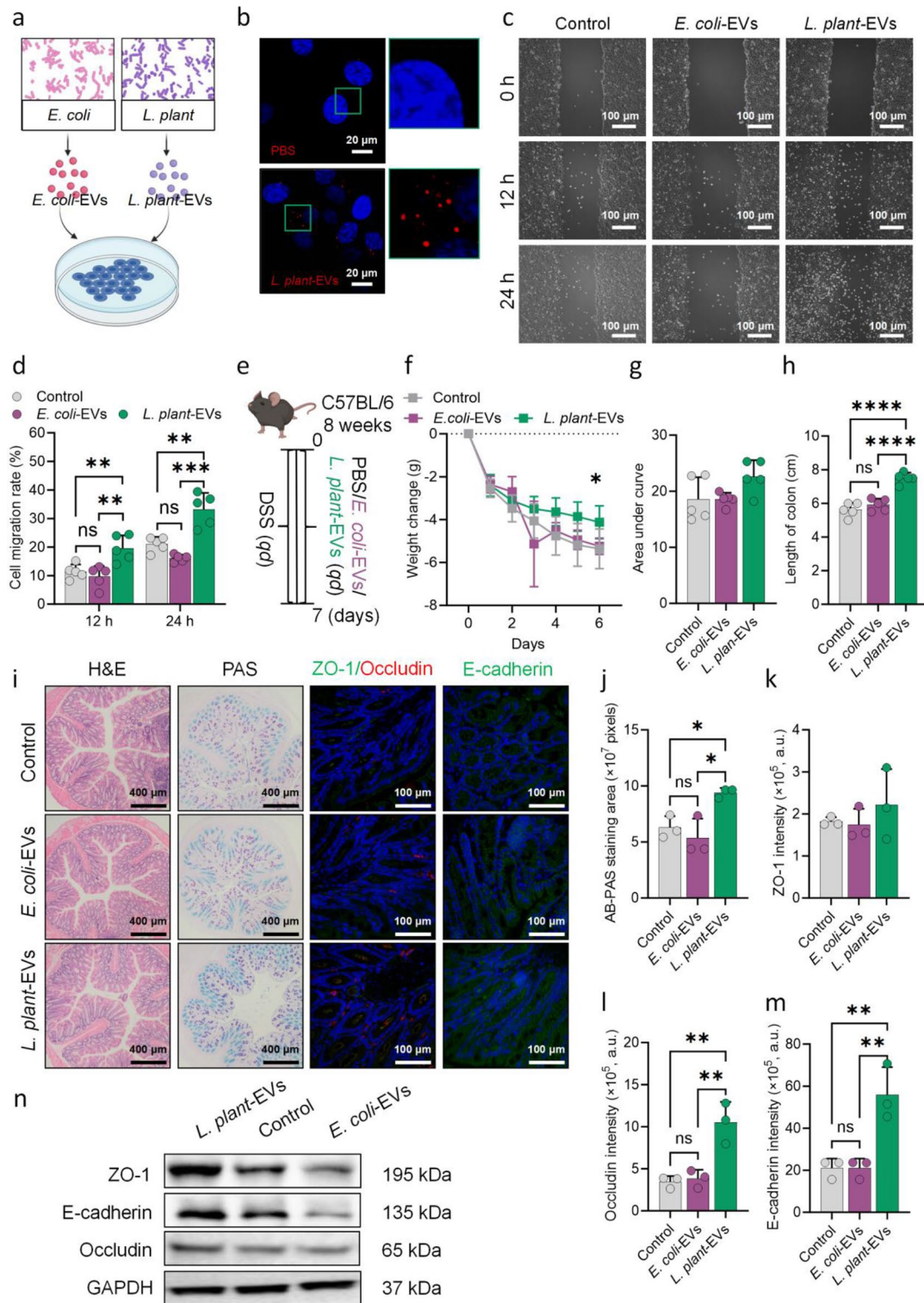


Fig. 2 Efficacy of *L. plant*-EVs in Alleviating IBD. **(a)** Schematic diagram illustrating the treatment of cells with *L. plant*-EVs. **(b)** Cellular uptake experiment, where blue fluorescence indicates DAPI staining, and red fluorescence marked *L. plant*-EVs labeled with CellMask. **(c, d)** Scratch assay conducted on NCM 460 cells to measure migration and healing capabilities at 12 h and 24 h ($n=5$). **(e)** Flow chart depicting the protocol for *L. plant*-EVs intervention in colitis mice. **(f, g)** Daily weight changes and area under the curve analyses in of the mice ($n=5$). **(h)** Measurement of colon length in each experimental group ($n=5$). **(i)** H&E stained colon sections, AB-PAS stained inner mucus layers of colon sections, and immunofluorescence staining for intestinal epithelial tight junction proteins. **(j-m)** Quantitative analysis of the mucus content secreted by goblet cells and the expression levels of the tight junction proteins Occludin, ZO-1, and E-cadherin ($n=3$). **(n)** Western blot analysis of E-cadherin, Occludin, and ZO-1 in the mouse colon. Two-way ANOVA was used to calculate the P values in **(f)**. One-way ANOVA was used to calculate the P values in **(d)**, **(g-h)** and **(j-m)**. * $P < 0.05$, ** $P < 0.01$, *** $P < 0.001$, **** $P < 0.0001$

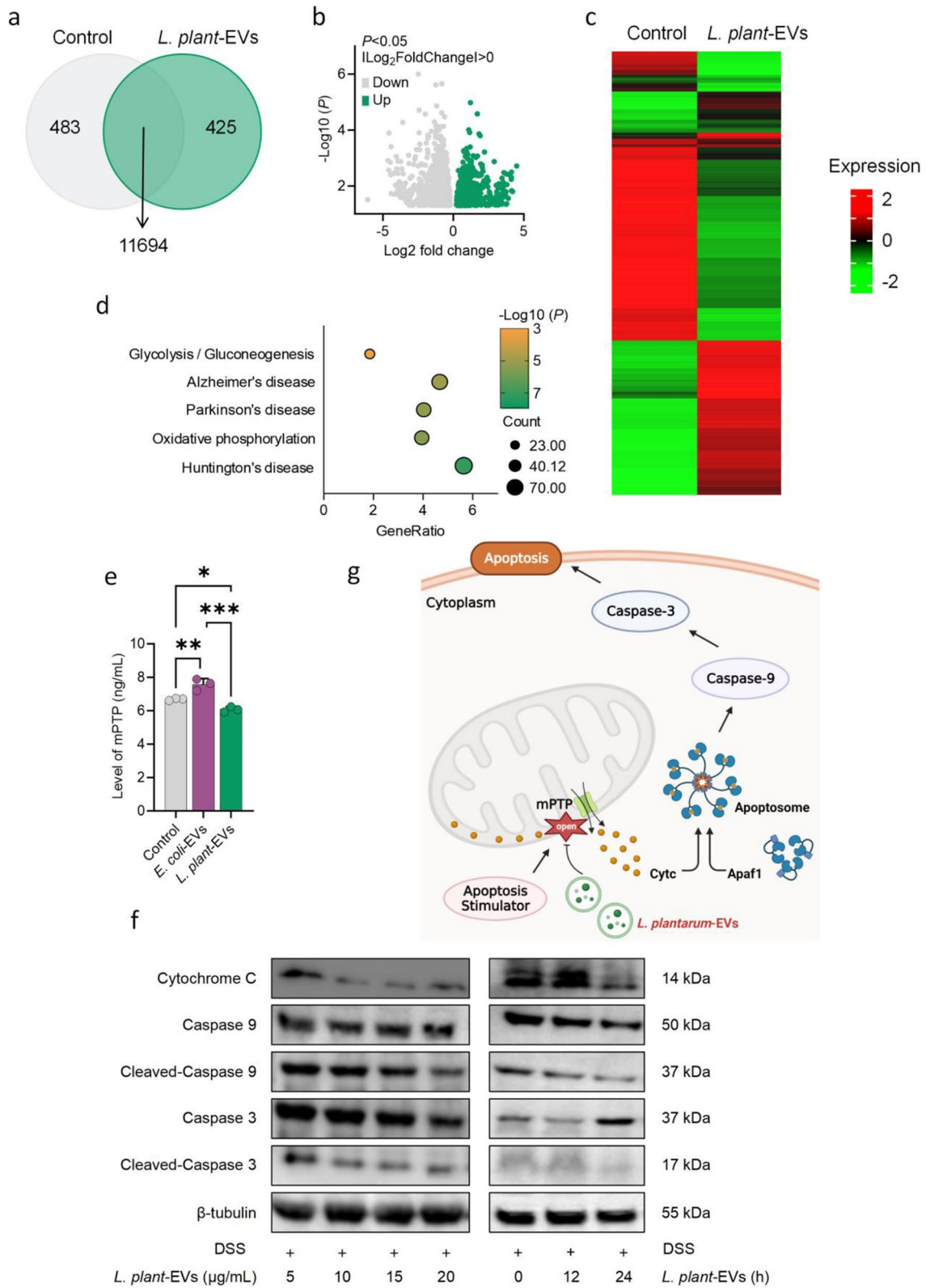


Fig. 3 (See legend on next page.)

(See figure on previous page.)

Fig. 3 Inhibition of Intestinal Epithelial Cell Apoptosis by *L. plant*-EVs via the mPTP-CytC-Caspase-9-Caspase-3 Axis. **(a)** Venn diagram showing differentially expressed genes (DEGs) in DSS-induced NCM 460 cells treated with *L. plant*-EVs compared to control cells. **(b)** Analysis of DEGs between the two groups using a volcano plot. **(c, d)** Gene Ontology (GO) enrichment analysis of the DEGs, with a heatmap displaying some DEGs associated with Huntington's disease. Differences in abundance were detected by using a multivariate statistical model ($p < 0.05$ [false-discovery rate-corrected], fold-change [FC] > 1.5 , MaAsLin2). **(e)** Measurement of mitochondrial permeability transition pore (mPTP) levels via enzyme-linked immunosorbent assay (ELISA). **(f)** Analysis of the apoptotic mechanisms in NCM 460 cells treated with 3% DSS and varying concentrations of *L. plant*-EVs for 24 h (left plot). Analysis of the apoptotic mechanisms in NCM 460 cells treated with 3% DSS and 20 $\mu\text{g/mL}$ *L. plant*-EVs at time points of 0, 12, and 24 h (right plot). **(g)** Kyoto Encyclopedia of Genes and Genomes (KEGG) analysis of the targeted pathway. One-way ANOVA was used to calculate the *P* values in **(e)**. * $P < 0.05$, ** $P < 0.01$, *** $P < 0.001$, and **** $P < 0.0001$

mPTP-CytC-Caspase pathway (Fig. 3f). To gain a deeper understanding of the dynamic changes in apoptotic protein expression, we analyzed these proteins at different time points (0, 12, and 24 h) following treatment with *L. plant*-EVs at a concentration of 20 $\mu\text{g/mL}$. The time-course analysis revealed a gradual reduction in CytC release and the expression levels of Cleaved-Caspase 3 and Cleaved-Caspase 9 over time (Fig. 3f). These findings provide additional evidence supporting the mechanistic involvement of the mPTP-CytC-Caspase pathway in *L. plant*-EVs-mediated alleviation of apoptosis. Complementing the biochemical analyses, we employed Annexin V-FITC/PI staining and flow cytometry to quantify apoptosis rates under different concentrations and time points. A significant dose-dependent decrease in apoptosis was observed with increasing concentrations of *L. plant*-EVs (Figure S4a, S4b). Similarly, the time-dependent analysis showed the lowest apoptosis rate at 24 h, corroborating the findings from the protein expression analysis (Figure S4c, S4d). The finding suggested that *L. plant*-EVs might inhibit the apoptosis of normal intestinal epithelial cells by downregulating the mPTP-CytC-Caspase-9-Caspase-3 signaling pathway. Such an action contributes to the maintenance of the intestinal barrier, offering therapeutic benefits for the treatment of IBD (Fig. 3g).

Watermelon increased *L. plantarum* colonization and BEVs release

Building on the findings, we delved deeper into the potential of dietary interventions in promoting colonization and the release of BEVs, with the ultimate goal of effectively managing IBD. Given that fruit is esteemed as a valuable source of prebiotics known to modulate the gut microbiota and enhance the colonization of probiotics [23, 24], we aimed to determine the most beneficial fruits for *L. plantarum*. For this purpose, pitaya, peach, and watermelon were chosen and incorporated into broth cultures for incubation. We selected pitaya, peeled peaches, and watermelon because they are commonly available and may offer varying benefits for managing colitis, with different levels of dietary fiber potentially influencing gut health and being suitable for IBD patients during remission [24]. Significantly, the watermelon supernatant accelerated the entry of *L. plantarum* into

the stationary phase of growth, whereas the other two groups did not have similar phenomena (Fig. 4a-c). The watermelon supernatant appeared to increase the proliferation of *L. plantarum* (Fig. 4d-f). In addition, the release of *L. plant*-EVs in the media containing watermelon supernatant also increased (Fig. 4g). These findings suggested that watermelon supernatant, distinctively compared to other fruits, had the ability to accelerate the growth of *L. plantarum* and the release of *L. plant*-EVs in vitro. To further explore whether watermelon can enhance the colonization in the host, volunteers were recruited and paired fecal samples were collected before and after watermelon consumption (Fig. 4h). While PCoA analysis revealed slight differences in microbial community structure between the pre-treatment and post-treatment groups (Fig. 4i), these changes were not accompanied by statistically significant shifts in diversity or richness, as indicated by the Shannon index, Simpson index, and Chao richness (Fig. 4j-l). Therefore, we found that while watermelon consumption may have caused changes in the abundance of specific bacteria, it did not significantly alter overall microbial diversity. Notably, the findings revealed an enrichment of *L. plantarum* in the human gut after watermelon consumption (Fig. 4m). In summary, our study demonstrated that watermelon could promote the colonization of *L. plantarum*.

Watermelon relieved IBD symptoms via the gut microbiota

Subsequently, we further explored whether watermelon could mitigate IBD by fostering the colonization of probiotics. Mice, following the depletion of their gut microbiota via antibiotics (Abx), received watermelon supernatant treatments (Fig. 5a). The outcomes revealed that, in DSS mice with an intact gut microbiota, there was a noticeable decline in both weight loss (Fig. 5b and c) and colonic shortening (Fig. 5d) after watermelon supernatant administration. Moreover, mice treated with watermelon supernatant, without prior gut microbiota clearance, displayed a normalization of goblet cell numbers and a decrease in inflammatory cell infiltration, culminating in augmented mucus production (Fig. 5e and f). However, in the mice pre-treated with antibiotics, DSS disrupted the intestinal barrier's tight junction proteins, and watermelon supernatant supplementation did not reverse this effect (Fig. 5e and f). Importantly, increases

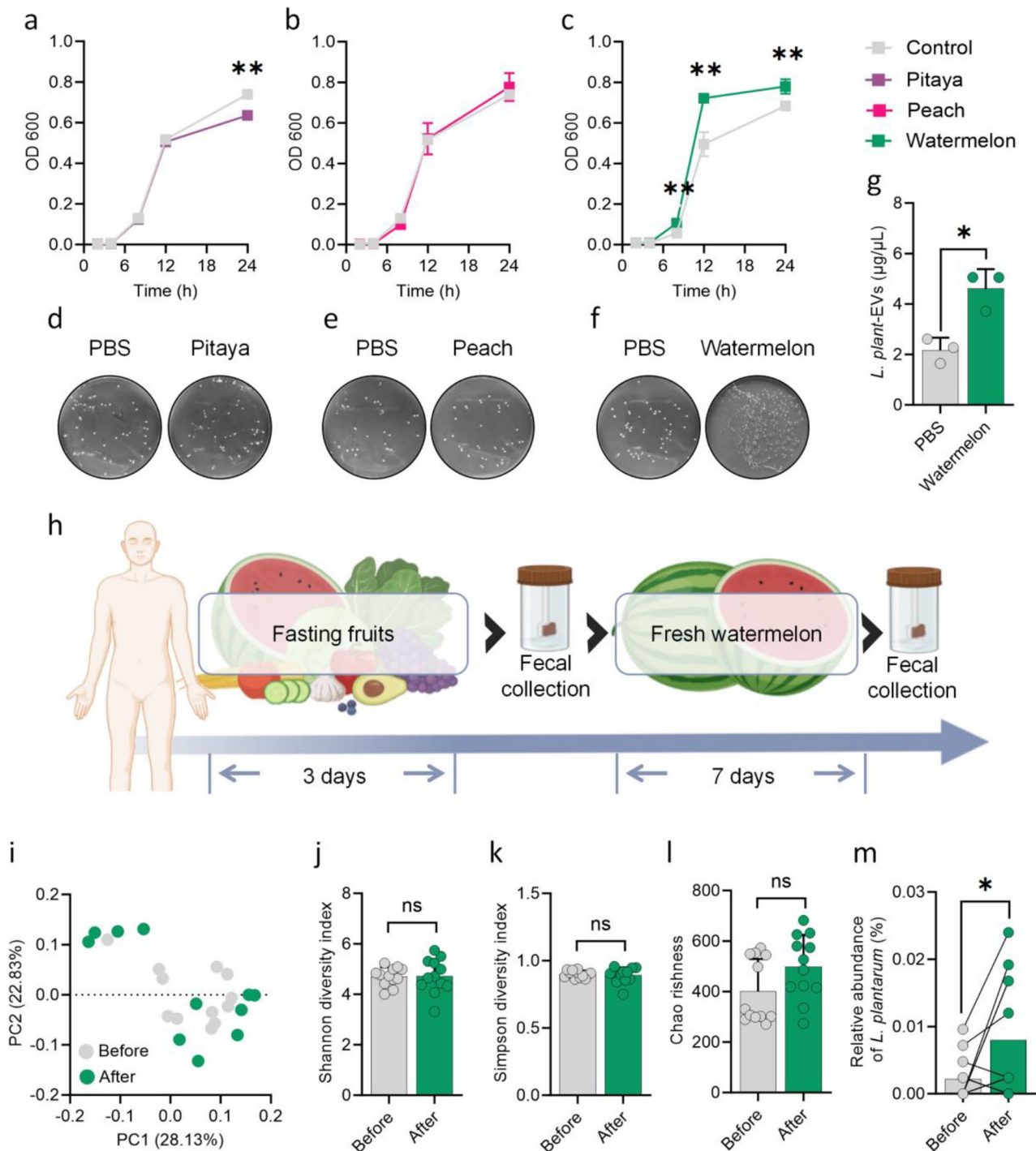


Fig. 4 Enhancement of *L. plantarum* Growth and BEVs Release by Watermelon. **(a-c)** Bacterial growth curves of *L. plantarum* following treatment with PBS, pitaya, peach, or watermelon. **(d-f)** Photomicrographs showing the colony numbers of *L. plantarum* after treatment with PBS, pitaya, peach, or watermelon. **(g)** Quantification of *L. plantarum*-EVs in culture medium supplemented with watermelon supernatant. **(h)** Process of fecal sample collection from volunteers undergoing watermelon dietary interventions. **(i)** Principal Coordinate Analysis (PCoA) plots illustrating microbiome diversity. **(j-l)** Analysis of microbial diversity ($n = 12$). **(m)** Comparative analysis of the relative abundance of intestinal *L. plantarum* in humans before and after watermelon treatment ($n = 6$). Two-way ANOVA was used to calculate p values in **(a-c)**. Student's t test was used to calculate the P values in **(g)** and **(m)**. Wilcoxon test was used to calculate the P values between before and after watermelon consumption in **(j-l)**. * $P < 0.05$, ** $P < 0.01$, *** $P < 0.001$, and **** $P < 0.0001$

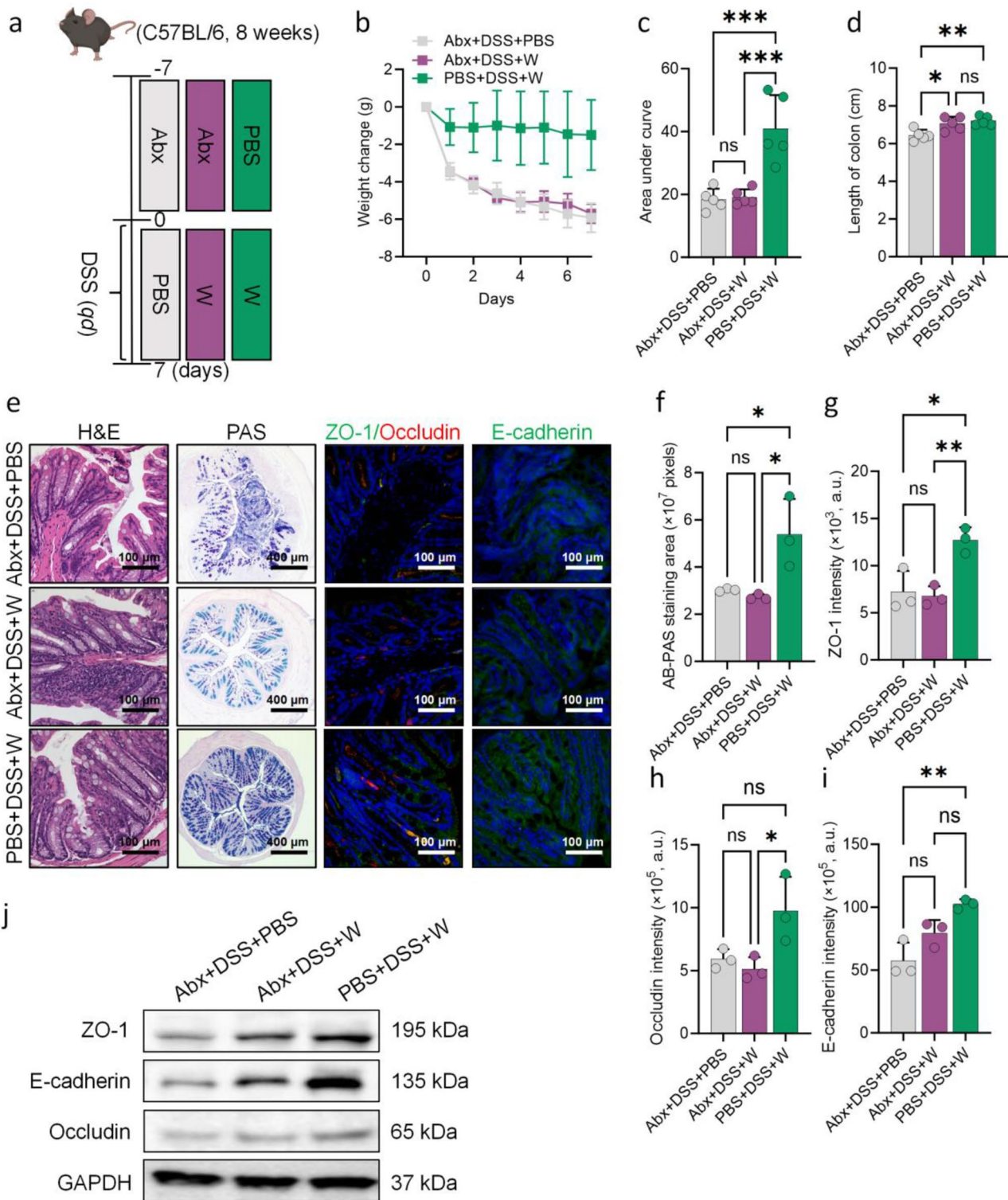


Fig. 5 Mitigation of IBD Symptoms by Watermelon via Modulation of the Gut Microbiota. **(a)** Flowchart of the animal experimental procedure. **(b, c)** Graphs showing daily weight changes and area under the curve analyses in mice, comparing groups with and without preemptive antibiotic-mediated clearance of intestinal flora, followed by DSS-induced colitis and treatment with watermelon supernatant ($n=5$). **(d)** Measurements of colon length from each experimental group ($n=5$). **(e)** H&E stained colon sections, AB-PAS stained inner mucus layers of colon sections, and immunofluorescence staining for intestinal epithelial tight junction proteins. **(f-h)** Quantitative analyses of mucus production by goblet cells and the expression levels of tight junction proteins Occludin, ZO-1, and E-cadherin ($n=3$). **(j)** Western blot analysis of E-cadherin, Occludin, ZO-1 in the mouse colon. Two-way ANOVA was used to calculate p values in **(b)**. One-way ANOVA was used to calculate the p values in **(c-d)** and **(f-i)**. * $P < 0.05$, ** $P < 0.01$, *** $P < 0.001$, and **** $P < 0.0001$

in the expression of Occludin, ZO-1, and E-cadherin were observed only in the group treated with watermelon supernatant that possessed intact intestinal flora, suggesting that the efficacy of watermelon supernatant in IBD treatment is contingent upon the modulation of the gut microbiota (Fig. 5g-i). This conclusion was confirmed by Western blot (Fig. 5j) and Figure S5a-c) and qPCR (Figure S5e-f). Additionally, we found that the combination of watermelon supernatant and *L. plantarum* (Figure S6a) enhanced the number of intestinal mucus-producing cells (Figure S6c and S6d) and the expression of tight junction proteins (Figure S6e-k) more effectively than watermelon supernatant alone in colon of DSS mice, despite no significant differences in colon length (Figure S6b). Collectively, these findings suggest that the therapeutic potential of watermelon in treating IBD is closely associated with its impact on the gut microbiota.

Discussion

Intestinal barrier dysfunction is a hallmark feature of IBD, referring to a disruption in the intestinal barrier structure that usually prevents harmful substances like bacteria, toxins, and undigested food particles from breaching the intestinal barrier and entering the bloodstream [25, 26], triggering inflammation and exacerbating the disease. Therefore, maintaining the integrity of the intestinal barrier is a critical therapeutic goal in IBD. Probiotics, defined as live microbes that confer health benefits when administered in adequate amounts, have gained considerable attention as a therapeutic approach to restore gut health and protect the intestinal barrier in IBD patients [27].

Probiotics have emerged as a multifaceted approach for protecting the intestinal mucosa, employing mechanisms such as inhibiting pathogenic bacteria, augmenting mucus secretion, upregulating tight junction proteins, modulating intestinal immune cells, and preventing epithelial cell apoptosis [28]. These mechanisms directly target the core pathological features of IBD. Consequently, regulating the intestinal environment through these mechanisms not only alleviates the symptoms of IBD but also potentially prevents disease recurrence or progression. By restoring the microbial balance, probiotics help suppress the growth of harmful microbes, including enteric pathogens such as *Escherichia coli* and *Clostridium difficile* [29]. *Lactobacillus reuteri* has been shown to protect the intestinal mucosal barrier integrity by moderately modulating the Wnt/ β -catenin signaling pathway, which is crucial for cell growth and repair, helping to avoid overactivation that could lead to inflammation [6]. Similarly, *Faecalibacterium prausnitzii* has been demonstrated to improve the tightness of the gut barrier among mice with DSS-induced colitis [30]. *Lactobacillus rhamnosus* has been shown to increase the expression of

both occludin and E-cadherin, further strengthening the epithelial barrier [31]. Administration of *Lactobacillus fermentum* among UC patients resulted in NF- κ B lowering regulation and additionally decreased the IL-6 and TNF- α levels [32].

Despite these promising effects, the exact molecular mechanisms and key components responsible for probiotics' efficacy remain to be fully elucidated. Emerging research underscores the significance of probiotics' active byproducts, including exopolysaccharides, short-chain fatty acids (SCFAs) [33], and BEVs [34, 35]. For instance, *Bifidobacterium longum* produce butyrate, which serves as an energy source for colonocytes, enhances epithelial cell integrity, and promotes anti-inflammatory responses [36]. These components exhibit an array of therapeutic properties, including anti-inflammatory, antitumor, antioxidant, and immunoregulatory effects. Our study investigated the therapeutic role of probiotic-BEVs on intestinal barrier function, particularly with respect to focusing on the reparative effect of *L. plant*-EVs.

The stability of the intestinal mucosal epithelium is contingent upon the equilibrium between cell proliferation and apoptosis. Disrupted balance, marked by accelerated apoptosis in colonic epithelial cells [37, 38], can severely impair intestinal barrier integrity, thus exacerbating IBD [39]. mPTP, residing between mitochondrial membranes, play a pivotal role in cell survival and apoptosis. Dysfunction in mitochondrial activity leads to mPTP opening, the subsequent release of CytC into the cytoplasm, and the activation of Caspase-9. This triggers a cascade involving Caspase-3, culminating in apoptosis [40, 41]. Our findings, derived from transcriptomic analyses and validated through western blotting and ELISA, revealed that *L. plant*-EVs downregulated the expression of apoptosis-related proteins such as mPTP, CytC, Caspase-9, and Caspase-3, suggesting their potential to increase in bolstering intestinal barrier integrity by curbing excessive epithelial cell apoptosis.

Moreover, the stable colonization of probiotics is integral to their functional efficacy. Dietary factors, particularly certain fruits, can significantly enhance probiotic colonization, thereby influencing disease management. Our comparative analysis of fecal samples from IBD patients, healthy individuals, and volunteers consuming watermelon daily, indicated that *L. plantarum*, potentially augmented by watermelon consumption, may play a crucial role in treating IBD. Additionally, watermelon supernatant was found to promote *L. plantarum* growth and *L. plant*-EVs release. These findings propose that dietary intervention, specifically through watermelon consumption, may foster an environment conducive to *L. plantarum* proliferation, thereby enhancing *L. plant*-EVs suggesting a novel approach to ameliorate intestinal barrier dysfunction.

In conclusion, our research investigated the protective effect of *L. plantarum* protective effect on the intestinal barrier and explored dietary interventions as a means of regulating the gut flora for intestinal repair. We demonstrated that watermelon consumption can increase *L. plantarum* proliferation and *L. plant*-EVs release, effectively protecting the intestinal barrier by mitigating apoptosis through the mPTP-CytC-Caspase-9-Caspase-3 pathway. These insights opened new avenues for adjunctive IBD therapies, spotlighting the potential of integrating probiotics and dietary modifications in treatment strategies.

Supplementary Information

The online version contains supplementary material available at <https://doi.org/10.1186/s12951-025-03280-7>.

Graphical abstract

Acknowledgements

Not applicable.

Author contributions

ZHO and QBL designed the study. YYW, XYH and QBL performed the animal experiments. XYH, YYW, QBL and CQY performed the in vitro experiments in human normal colonic epithelial cells and *L. plantarum*. XYH, YYW, and XXH performed the Western Blot and enzyme-linked immunosorbent assays. YYW and PPW collected samples and clinical information from healthy donors and colitis patients. ZHO and QBL performed the data analyses. XYH, YYW, QBL, XXH, and ZHO wrote the manuscript. ZHO, LZ and BST supervised the project.

Funding

This work was supported by the National Science Fund for Distinguished Young Scholars (82025024); the Key project of the National Natural Science Foundation of China (82230080); the National Natural Science Foundation of China (82302593, 82272438); the Guangdong Natural Science Fund for Distinguished Young Scholars (2023B1515020058); the Natural Science Foundation of Guangdong Province (2021A1515011639, 2023A1515012512); the Major State Basic Research Development Program of the Natural Science Foundation of Shandong Province in China (ZR2020ZD11); the Outstanding Youths Development Scheme of Nanfang Hospital, Southern Medical University (2022J001).

Data availability

No datasets were generated or analysed during the current study.

Declarations

Ethics approval and consent to participate

All mouse experiments in this study were approved by the Committee on the Use of Live Animals in Teaching and Research at the Southern Medical University (approval number: SMUL2022002). The sample collection protocol was approved by the Ethics Committee of Nanfang Hospital, Southern Medical University (approval number: NFEC-2022-001).

Consent for publication

Not applicable.

Competing interests

The authors declare no competing interests.

Author details

¹Department of Laboratory Medicine, Nanfang Hospital, Southern Medical University, Guangzhou 510515, China

²Ganzhou Hospital-Nanfang Hospital, Southern Medical University, Guangzhou, China

Received: 4 February 2025 / Accepted: 24 February 2025

Published online: 20 March 2025

References

1. Ananthakrishnan AN. Epidemiology and risk factors for IBD. *Nat Rev Gastroenterol Hepatol.* 2015;12(4):205–17.
2. Caruso R, Lo BC, Núñez G. Host-microbiota interactions in inflammatory bowel disease. *Nat Rev Immunol.* 2020;20(7):411–26.
3. Baumgart DC, Le Berre C. Newer biologic and Small-Molecule therapies for inflammatory bowel disease. *N Engl J Med.* 2021;385(14):1302–15.
4. Carter MJ, Lobo AJ, Travis SP. Guidelines for the management of inflammatory bowel disease in adults. *Gut.* 2004;53(Suppl 5):V1–16.
5. Preidis GA, Versalovic J. Targeting the human Microbiome with antibiotics, probiotics, and prebiotics: gastroenterology enters the metagenomics era. *Gastroenterology.* 2009;136(6):2015–31.
6. Wu H, Xie S, Miao J, et al. *Lactobacillus reuteri* maintains intestinal epithelial regeneration and repairs damaged intestinal mucosa. *Gut Microbes.* 2020;11(4):997–1014.
7. Han JX, Tao ZH, Wang JL, et al. Microbiota-derived Tryptophan catabolites mediate the chemopreventive effects of Statins on colorectal cancer. *Nat Microbiol.* 2023;8(5):919–33.
8. Yin J, Sun W, Yu X, et al. *Lacticaseibacillus rhamnosus* TR08 alleviated intestinal injury and modulated microbiota dysbiosis in septic mice. *BMC Microbiol.* 2021;21(1):249.
9. Sartorio MG, Pardue EJ, Feldman MF, Haurat MF. Bacterial outer membrane vesicles: from discovery to applications. *Annu Rev Microbiol.* 2021;75:609–30.
10. Gul L, Modos D, Fonseca S, et al. Extracellular vesicles produced by the human commensal gut bacterium *Bacteroides thetaiotaomicron* affect host immune pathways in a cell-type specific manner that are altered in inflammatory bowel disease. *J Extracell Vesicles.* 2022;11(1):e12189.
11. Xie J, Cools L, Van Imschoot G, et al. *Helicobacter pylori*-derived outer membrane vesicles contribute to Alzheimer's disease pathogenesis via C3-C3aR signalling. *J Extracell Vesicles.* 2023;12(2):e12306.
12. Yáñez-Mó M, Siljander PR, Andreu Z, et al. Biological properties of extracellular vesicles and their physiological functions. *J Extracell Vesicles.* 2015;4:27066.
13. Ou Z, Situ B, Huang X, et al. Single-particle analysis of Circulating bacterial extracellular vesicles reveals their biogenesis, changes in blood and links to intestinal barrier. *J Extracell Vesicles.* 2023;12(12):e12395.
14. Wen M, Wang J, Ou Z, et al. Bacterial extracellular vesicles: A position paper by the microbial vesicles task force of the Chinese society for extracellular vesicles. *Interdisciplinary Med.* 2023;1(3):e12046.
15. Nahui Palomino RA, Vanpouille C, Costantini PE, Margolis L. Microbiota-host communications: bacterial extracellular vesicles as a common Language. *PLoS Pathog.* 2021;17(5):e1009508.
16. Toyofuku M, Schild S, Kaparakis-Liaskos M, Eberl L. Composition and functions of bacterial membrane vesicles. *Nat Rev Microbiol.* 2023;21(7):415–30.
17. Wang X, Lin S, Wang L, et al. Versatility of bacterial outer membrane vesicles in regulating intestinal homeostasis. *Sci Adv.* 2023;9(11):eade5079.
18. Molina-Tijeras JA, Gálvez J, Rodríguez-Cabezas ME. The Immunomodulatory properties of extracellular vesicles derived from probiotics: A novel approach for the management of Gastrointestinal diseases. *Nutrients* 2019; 11(5).
19. Ou Z, Deng L, Lu Z, et al. Protective effects of *Akkermansia muciniphila* on cognitive deficits and amyloid pathology in a mouse model of Alzheimer's disease. *Nutr Diabetes.* 2020;10(1):12.
20. Xie J, Haesebrouck F, Van Hoecke L, Vandenbroucke RE. Bacterial extracellular vesicles: an emerging avenue to tackle diseases. *Trends Microbiol.* 2023;31(12):1206–24.
21. Lim Y, Kim HY, An SJ, Choi BK. Activation of bone marrow-derived dendritic cells and CD4(+) T cell differentiation by outer membrane vesicles of periodontal pathogens. *J Oral Microbiol.* 2022;14(1):2123550.
22. Kim HJ, Kim YS, Kim KH, et al. The Microbiome of the lung and its extracellular vesicles in nonsmokers, healthy smokers and COPD patients. *Exp Mol Med.* 2017;49(4):e316.
23. Kulp A, Kuehn MJ. Biological functions and biogenesis of secreted bacterial outer membrane vesicles. *Annu Rev Microbiol.* 2010;64:163–84.

24. Jakubczyk D, Leszczyńska K, Górka S. The effectiveness of probiotics in the treatment of inflammatory bowel disease (IBD)—A critical review. *Nutrients*. 2020; 12(7).
25. Dong L, Xie J, Wang Y, et al. Mannose ameliorates experimental colitis by protecting intestinal barrier integrity. *Nat Commun*. 2022;13(1):4804.
26. Tulkens J, Vergauwen G, Van Deun J, et al. Increased levels of systemic LPS-positive bacterial extracellular vesicles in patients with intestinal barrier dysfunction. *Gut*. 2020;69(1):191–3.
27. Lee SH. Intestinal permeability regulation by tight junction: implication on inflammatory bowel diseases. *Intest Res*. 2015;13(1):11–8.
28. Kang Y, Kang X, Yang H, et al. *Lactobacillus acidophilus* ameliorates obesity in mice through modulation of gut microbiota dysbiosis and intestinal permeability. *Pharmacol Res*. 2022;175:106020.
29. Stoeva MK, Garcia-So J, Justice N, et al. Butyrate-producing human gut symbiont, *Clostridium Butyricum*, and its role in health and disease. *Gut Microbes*. 2021;13(1):1–28.
30. Mohebbali N, Weigel M, Hain T, et al. *Faecalibacterium Prausnitzii*, *Bacteroides faecis* and *Roseburia intestinalis* attenuate clinical symptoms of experimental colitis by regulating Treg/Th17 cell balance and intestinal barrier integrity. *Biomed Pharmacother*. 2023;167:115568.
31. Laval L, Martin R, Natividad JN, et al. *Lactobacillus rhamnosus* CNCM I-3690 and the commensal bacterium *Faecalibacterium prausnitzii* A2-165 exhibit similar protective effects to induced barrier hyper-permeability in mice. *Gut Microbes*. 2015;6(1):1–9.
32. Wang K, Sun J, Zhao J, et al. Immunomodulatory activity and protective effect of a capsular polysaccharide in *Caenorhabditis elegans*, isolated from *Lactobacillus fermentum* GBJ. *Int J Biol Macromol*. 2023;253(Pt 7):127443.
33. Parada Venegas D, De la Fuente MK, Landskron G, et al. Short chain fatty acids (SCFAs)-Mediated gut epithelial and immune regulation and its relevance for inflammatory bowel diseases. *Front Immunol*. 2019;10:277.
34. Chen Y, Ou Z, Pang M, et al. Extracellular vesicles derived from *Akkermansia muciniphila* promote placentation and mitigate preeclampsia in a mouse model. *J Extracell Vesicles*. 2023;12(5):e12328.
35. Zheng X, Huang W, Li Q, et al. Membrane protein Amuc_1100 derived from *Akkermansia muciniphila* facilitates lipolysis and Browning via activating the AC3/PKA/HSL pathway. *Microbiol Spectr*. 2023;11(2):e0432322.
36. Budden KF, Gellatly SL, Vaughan A et al. Probiotic *Bifidobacterium longum* subsp. *longum* protects against cigarette Smoke-Induced inflammation in mice. *Int J Mol Sci* 2022; 24(1).
37. Farkas AE, Capaldo CT, Nusrat A. Regulation of epithelial proliferation by tight junction proteins. *Ann N Y Acad Sci*. 2012;1258:115–24.
38. Vereecke L, Beyaert R, van Loo G. Enterocyte death and intestinal barrier maintenance in homeostasis and disease. *Trends Mol Med*. 2011;17(10):584–93.
39. Li X, Li Q, Xiong B, Chen H, Wang X, Zhang D. Discoidin domain receptor 1 (DDR1) promote intestinal barrier disruption in ulcerative colitis through tight junction proteins degradation and epithelium apoptosis. *Pharmacol Res*. 2022;183:106368.
40. Tian M, Dong B, Zhang Z, Yin J, Lin W. Permeability-Controlled probe for directly visualizing the opening of mitochondrial permeability transition pore in native status. *Anal Chem*. 2022;94(13):5255–64.
41. Li Z, Guo D, Yin X, et al. Zinc oxide nanoparticles induce human multiple myeloma cell death via reactive oxygen species and Cyt-C/Apaf-1/Caspase-9/Caspase-3 signaling pathway in vitro. *Biomed Pharmacother*. 2020;122:109712.

Publisher's note

Springer Nature remains neutral with regard to jurisdictional claims in published maps and institutional affiliations.